Chemical Engineering Journal 162 (2010) 97–105

Contents lists available at ScienceDirect

Chemical Engineering Journal

journal homepage: www.elsevier.com/locate/cej

Thallium adsorption onto polyacryamide–aluminosilicate composites: A Tl isotope tracer study

Zeynep Mine Şenol, Ulvi Ulusoy*

Cumhuriyet University, Department of Chemistry, Sivas 58140, Turkey

ARTICLE INFO

Article history:
Received 11 February 2010
Received in revised form 4 May 2010
Accepted 5 May 2010

Keywords:
Thallium
Adsorption
Aluminosilicate
Composite
Isotope tracer

ABSTRACT

Adsorptive features of the composites of polyacrylamide (PAAm) and bentonite (B), and zeolite (Z) were investigated for Tl^+ and Tl^{3+}.

Langmuir monolayer adsorption capacities for the corresponding ions were 1.85 and 0.97 mol kg^{-1} for PAAm–Z and 0.36 and 0.16 mol kg^{-1} for PAAm–B. The values of enthalpy and entropy changes were positive for both composites and ions. The compatibility of the second order adsorption kinetics implied that the rate-controlling step was concentration dependent; the sorption process was ion exchange. High adsorption rate was found for both composites; the time required for adsorption of half of Tl^+ concentrations was 7 min.

In the presence of both ions, PAAm–B was more selective for Tl^{3+} than PAAm–Z. The reusability tests for Tl^+ for five uses proved that the composites were reusable after complete recovery of the loaded ion. The values of Tl^+ adsorption onto PAAm–Z from solutions containing Fe^{3+}, Pb^{2+}, Zn^{2+} confirmed that the effect of the presence of these ions on Tl^+ extraction was not significant. Although Tl^+ sorption decreased with increasing ionic strength ($CaCl_2$) of the medium, the results of adsorption from sea water containing 5×10^{-6} mol L^{-1} (1 mg L^{-1}) of Tl^+ ascertained that the composites still adsorbed about 10% of Tl.

1. Introduction

Thallium (Tl) classified in the group III A of the periodic chart has two comparatively stable state ions, monovalent (Tl^+; thallous) and trivalent (Tl^{3+}; thallic). Tl^+ resembles to group I cations (Pb^{2+}, $Hg_2{}^{2+}$ and Ag^+) and also to K^+, Rb^+ and Cs^+ of the alkali-metal ions [1]. Monovalent Tl is more stable than trivalent Tl analogues in aqua solution at neutral pH. The dissolved Tl in sea water (10–100 pmol kg^{-1}) contains only about 1–5% of Tl in trivalent state. In rocks, it is concentrated in plagioclase or in K^+-minerals such as K-feldspars and biotite. Thallium is observed to be a part of sulfide melts and it is enriched in some sulfide minerals [2].

Thallium in both states is toxic and acts as a cumulative poison. High Tl^+ concentration in the blood agglutinates and lyses erythrocytes. Tl^{3+} has a strong capacity to complex with citrates, glutamates and albumin. Lethal dose (LD_{100}) of Tl^+ by subcutaneous or intravenous injection is 12–15 mg kg^{-1} in dogs, 20–25 mg kg^{-1} in rats and 8–10 mg kg^{-1} in humans [3,4]. Tl is introduced into the environment mainly as waste from the production of Zn, Cd and Pb and by combustion of coal [5]. The U.S. Environmental Protection Agency (EPA) standards for Tl is 2 μg L^{-1} in drinking water, 4 μg L^{-1} in sea water, 140 μg L^{-1} in wastewaters and 0.1 mg m^{-3} in stack gas.

Industrial uses of Tl and its compounds are in the manufacture of imitation jewelry, low-temperature thermometers, ceramic semiconductor materials, scintillation counters for radioactivity measurements and optical lenses. Tl compounds are used in IR spectrometers, optical systems, semiconductor and laser industry, scintillographic imaging, super conductivity, coloring glass and as a molecular probe to emulate the biological function of alkali-metal ions [6].

Because of the toxicity and the industrial importance, removal/recovery of Tl in waste and contaminated water has been among major concerns of process industries [7]. The EPA indicated that only two industrial removal technologies exist for recovering thallium from process solutions: oxidative precipitation of thallichydroxide and reductive cementation of thallium using elemental zinc as the precipitant the best one of which is the chemical oxidation of thallium followed by chemical precipitation with hydroxide compounds, settling, and filtration (http://www.epa.gov/minewastetechnology/annual/annual2004/mwtp2004annualrpt.pdf, last visited in 29.04.2010). Due to the strong tendency of Tl^{3+} to form a complex, the interest of investigations is generally given to its extraction by complex forming reagents as reported by Nascimento and Schwedt [8], Gidwani et al. [9], Chung et al. [7], Zhang et al. [10], and Rajesh and Subramanian

Abbreviations: B, bentonite; Z, zeolite; PAAm, polyacrylamide; PAAm–B/Z, the composites of polyacrylamide and bentonite/zeolite; DR, Dubinin–Radushkevich.

* Corresponding author. Tel.: +90 346 2191010x1623; fax: +90 346 2191186.
E-mail address: ulusoy@cumhuriyet.edu.tr (U. Ulusoy).

1385-8947/$ – see front matter © 2010 Elsevier B.V. All rights reserved.
doi:10.1016/j.cej.2010.05.005

[11]. The researches performed by Chang et al. [12] and Jacobson et al. [13] have considered the preconcentration of Tl^+ by chelating resin. Despite the considerable success achieved through those studies, especially the high cost beside opinions related to efficacy and practicality have remained controversial.

The adsorption processes are generally known to be one of the most effective techniques for the removal/recovery of metal ions. Adsorbents should have strong affinity and high loading capacity for targeted metal ions. While synthetic ion-exchange resins are expensive to use on a large scale, natural materials such as clay and zeolite are classified among the low-cost adsorbents [14–16]. The aggregation and coagulation of these minerals under varying conditions of temperature and electrolytes which lead to variations in flow properties of these minerals is an undesired feature for their practical use as adsorbents [17–19]. Having a composite of a mineral and a hydrogel polymer, in which the mineral is dispersed in the polymer network, may enable the use of mineral itself as an adsorbent confined in an isolated and practically usable medium in aquatic solutions. The particles embedded in a network may also strengthen the gel and prevent its collapse in bad solvents. However, the practical applicability of this approach has been shown for the composite of bentonite (B) or zeolite (Z) and polyacrylamide (PAAm) for adsorption of Fe^{3+}, Zn^{2+}, $UO_2{}^{2+}$ and Pb^{2+} [20]. The applications were also confirmed for adsorption of naturally occurring radionuclide at pmol L^{-1} levels, including ^{208}Tl [21,22].

The aim of this investigation was to introduce PAAm–B and PAAm–Z composites for practical use of B and Z in Tl (in both oxidation states) adsorption procedures. The preparation and characterization of PAAm–B/Z and its adsorptive features with reference to the dependency on concentration, temperature and time were investigated. Additional considerations were also given to the reusability and Tl^+/Tl^{3+} selectivity of the composites, the effect of the presence of Fe^{3+}, Pb^{2+} and Zn^{2+}, ionic strength and sea water on Tl adsorption.

2. Experimental

2.1. Reagents

Acrylamide (AAm) monomer, N,N′-methylenebisacrylamid, N,N,N′,N′-tetramethylethylenediamine and TlCl were purchased from Aldrich. Merck was the supplier of 4-(2-pyridylazo)-resorcinol (PAR). Sodium bentonite (98% in purity) with 0.80 mol kg^{-1} cation exchange capacity [20] was obtained from Sigma. Nitrate salts of Fe, Zn and Pb (Merck) were used in studies related to these ions. All chemicals used were of analytical reagent grade.

Zeolite was obtained from Central North Anatolian occurrences associated with Eocene submarine volcanism. The mineral is composed of 90% zeolite, as clinoptilolite$\{(Na,K)_6{\cdot}[Al_6Si_{30}O_{72}]{\cdot}24H_2O\}$and mordenite$\{Na_3KCa_2{\cdot}[Al_8Si_{40}O_{96}]{\cdot}28H_2O\}$, 5% quartz, 5% feldspar and smectite in trace level. The ratio of SiO_2/Al_2O_3 is 4.7, which suggests that the zeolite is clinoptilolite with reference to the classification of International Mineralogical Association [18]. The zeolite rocks were crashed, ground and sieved to an average 100 mesh size. No pre-treatment was applied to the chemicals, clay and zeolite.

^{201}Tl was used as the radioactive tracer, the residue in bottles of serum physiologic containing $^{201}TlCl$ (Monrol) after the use of medical purpose was obtained from the Nuclear Medicine Department.

All experiments were always performed in duplicates ±5% was the limit of experimental error of each duplicates, any experiment resulted in higher than this limit was repeated. Time to attain equilibration between solution and adsorbent was chosen to be 24 h, as appropriate to the convention, despite the fact that the studies related to kinetics implied a shorter time than this duration (see below). The study temperature was always 298 K unless otherwise indicated.

2.2. Preparation of PAAm–B and PAAm–Z

PAAm–B or PAAm–Z was prepared by direct polymerization of AAm monomer in the clay and zeolite suspensions [23]. The final composition of the composites had 2:1 mass ratio of PAAm to the clay or zeolite. The gels were washed with distilled water until neutral pH was attained, dried at ambient temperature, ground and sieved to a particle size in the range of 50–75 mesh, and stored in a container. To avoid the inter-sample variations, one batch of PAAm–B and PAAm–Z was prepared at once to conduct the overall investigation. The hybrid formation of the composites was confirmed by means of FT-IR and XRD analysis [20,23]. BET and porosity measurements (Quantachrome, Quantachrome Instruments) and SEM photographs were of the additional characterizations reported herein.

The preliminary adsorption investigation for PAAm proved that PAAm was inert for the ions studied.

2.3. Preparation of ^{201}Tl tagged Tl^+/Tl^{3+} solutions and determination

200 μL of $^{201}TlCl$ residue with 1 MBq activity was diluted to provide ≈100 Bq mL^{-1} from which 1 mL of fractions was used as spike for each 10 mL of Tl solutions. Final activity of the solutions studied was ≈10 Bq mL^{-1}.

Tl^+ solutions were prepared by dissolving TlCl in distilled water and spiked with ^{201}Tl. HNO_3 and H_2O_2 were used as oxidizing reagents for the preparation of Tl^{3+} solutions. The required amount of TlCl spiked with ^{201}Tl tracer was dissolved in conc. HNO_3 by heat and a few drops of H_2O_2 were added during the evaporation. The procedure was repeated until the completion of oxidation. This was ensured by the PAR test; a 50 μL fraction of solution was added onto 3 mL of the PAR reagent (3.5×10^{-3} mol L^{-1} of PAR in 0.7 mol L^{-1} of Tris/HCl at pH 8–9) and the absorbance of the formed Tl^{3+} complex was measured at 520 nm. Special attention was paid to the freshness of Tl solutions due to its instability under light and oxidizing effect of air [24]. Stability of Tl^{3+} was ensured by the PAR test in any stage of the study.

A gamma spectrometer [NaI(Tl) detector combined with a EG&G ORTEC multi-channel analyzer and software, MAESTRO 32, MCA Emulator, USA] was employed for activity measurements of ^{201}Tl. The accumulated counts under X-ray at 76 keV were evaluated for the determinations, the gammas at 135 and 167 keV were also considered for justification. Time for counting of samples was usually 2000 s to collect at least 10,000 counts to provide 1% coefficient of variance.

2.4. pH dependence of Tl adsorption

Initial pH of 10 mL fractions of Tl solutions containing 4.9×10^{-3} mol L^{-1} (1000 mg L^{-1}) of Tl^+ or Tl^{3+} (spiked with ^{201}Tl) were adjusted to 1–5 for Tl^+ and 1–3 for Tl^{3+} by addition of 0.1 mol L^{-1} HCl. The adjustment of Tl^{3+} was ceased at pH = 3, since Tl^{3+} precipitates over this pH [1]. 0.1 g of adsorbents were added into the solutions and agitated in a thermostatic water bath for 24 h. After centrifugation at 1000 rpm for 3 min, the adsorbed amounts were determined by activity comparison of 5 mL fractions of the supernatants and the reference (Tl solutions not interacted with the adsorbents).

The same experimental procedure (interaction time, temperature, agitation and centrifugation) and method for Tl^+/Tl^{3+}

determination were applied to the other adsorption studies unless otherwise specified. Tl^+ solutions were used as prepared from its salt (TlCl) having a pH in the range of 5.5–3.5 for 10^{-5}–10^{-2} mol L^{-1} (2–2000 mg L^{-1}) of Tl^+. The adjusted pH of Tl^{3+} solutions was 3.

2.5. Concentration dependence of Tl adsorption

The concentration dependence of adsorption was investigated for Z beside PAAm–B and PAAm–Z but not for B due to its distinct aggregation/coagulation features.

0.1 g fractions of PAAm–B, PAAm–Z and Z were equilibrated with 10 mL of 10^{-5}–10^{-2} mol L^{-1} (2–2000 mg L^{-1}) Tl^+ or Tl^{3+} solutions.

2.6. Temperature dependence of Tl adsorption

The effect of temperature on adsorption for the determination of thermodynamic parameters was studied for three temperatures: 278, 298 and 313 K. 0.1 g fractions of the composites were equilibrated with 5×10^{-3} mol L^{-1} (1000 mg L^{-1}) of Tl^+ or Tl^{3+}.

2.7. Adsorption kinetics

40 mL of 5×10^{-3} mol L^{-1} (1000 mg L^{-1}) of Tl^+ or Tl^{3+} was added onto 0.4 g of PAAm–B and PAAm–Z. 500 μL fractions of solution were withdrawn for 4 h starting immediately after the solution–solid contact and continued with time intervals. Sampling for 4 h was enough since the adsorption did not change about 2 h after the contacts.

2.8. Reusability

0.1 g of PAAm–B and PAAm–Z in polypropylene columns (100 mm height × 10 mm i.d., with a glass-wool over its stopcock) were equilibrated with 10 mL of 5×10^{-3} mol L^{-1} Tl^+ for 2 h (sufficient time for the completion of adsorption after kinetic studies) and the adsorbed amounts were determined. The contents of columns were eluted with 30 mL of 0.25 mol L^{-1} HCl with a flow rate of 1 mL min^{-1}. The recovery of Tl^+ with HCl was determined. The columns were then reconditioned with 20 mL of distilled water until the effluents had around neutral pH. Each sample was subjected to the same procedure for 4 sequential times to provide five uses in total. The reusability of the composites was tested for only Tl^+, since Tl^{3+} precipitated at neutral pH [1].

2.9. Tl^+/Tl^{3+} selectivity and Tl adsorption in the presence of Fe^{3+}, Pb^{2+} and Zn^{2+}

0.1 g fractions of PAAm–B and PAAm–Z were equilibrated with 10 mL of Tl solution in combination of 5 mL of 5×10^{-3} mol L^{-1} Tl^+ spiked with ^{201}Tl and 5 mL of untagged 5×10^{-3} mol L^{-1} Tl^{3+} (pH = 3) The equilibration of solid-solution system was also investigated for tagged Tl^{3+} and untagged Tl^+ at the same ion concentrations.

Since Tl is mostly abundant in sulfide minerals such as pyrite (FeS_2), galena (PbS) and sphalerite (ZnS), Tl^+ and Tl^{3+} adsorption in the presence of Fe^{3+}, Pb^{2+} and Zn^{2+} either individually or all three ions were tested (pH = 3). 0.1 g of the composites were equilibrated with 10 mL of 5×10^{-3} mol L^{-1} of Fe^{3+}, Pb^{2+} and Zn^{2+} solutions (prepared from their nitrate salts) containing Tl^+ or Tl^{3+} at equivalent and diluted concentrations to provide 1/10 and 1/100 ratios of [Tl]/[5×10^{-3} mol L^{-1} M^{z+}].

2.10. The effect of ionic strength and Tl^+ adsorption from sea water

0.1 g fractions of the composites were interacted with 10 mL of 5×10^{-3} mol L^{-1} of Tl^+ (pH≈5) containing 0.01–0.1 mol L^{-1} $CaCl_2$. Tl contents of the equilibrium solutions were then determined.

TlCl solutions were prepared in sea water (pH = 6.5) to provide 5×10^{-6}–5×10^{-4} mol L^{-1} (1, 10, 50 and 100 mg L^{-1}) of Tl^+. 0.1 g fractions of the composites were equilibrated with 10 mL of these solutions.

2.11. Data processing

The following equations were used for data evaluation (the related symbols and units were provided in the text box below).

The fractional transfer of ^{201}Tl to solid phase from Tl solutions and the adsorbed amounts onto the mineral components of the composites were derived from

$$F = \frac{A_i - A_e}{A_i} \tag{1}$$

$$Q = \left[\frac{FxC_i xV}{W}\right] \tag{2}$$

The experimentally obtained isotherms were evaluated with reference to their compatibility to Langmuir, Freundlich and Dubinin–Radushkevich (DR) models defined with:

$$Q = \frac{K_L X_L C_e}{1 + K_L C_e} \tag{3}$$

$$Q = X_F C_e^n \tag{4}$$

$$Q = X_{DR} e^{-K_{DR}\varepsilon^2} \tag{5}$$

In accordance with the DR model, Polanyi potential (Eq. (6)) and free energy (Eq. (7)) required to transfer one mole of ion from the infinity in the solution to the solid surface were then derived from

$$\varepsilon = RT \ln\left(1 + \frac{1}{C_e}\right) \tag{6}$$

$$E = (-2K_{DR})^{-1/2} \tag{7}$$

As suggested by Doğan and Alkan [25], Langmuir isotherms were further considered to predict if the composites were 'favorable' in view of the dimensionless factor (Eq. (8)) and to calculate the weight of composites for removing Tl from hypothetic solutions (Eq. (9)) by

$$R_D = \frac{1}{1 + K_L C_e} \tag{8}$$

$$\frac{W}{V} = \frac{C_i - C_e}{K_L X_L C_e/(1 + K_L C_e)} \tag{9}$$

To elucidate the temperature dependence of adsorption, the distribution coefficients (K_d) were derived from $K_d = Q/C_e$ for each temperature and '$\ln K_d$' was depicted against $1/T$ to provide adsorption enthalpy and entropy from the slopes ($\Delta H/R$) and intercepts ($\Delta S/R$) of the depictions with reference to:

$$\ln K_d = \frac{\Delta S}{R} - \frac{\Delta H}{RT} \tag{10}$$

and ΔG values for 298 K were then calculated from:

$$\Delta G = \Delta H - T\,\Delta S \tag{11}$$

Equations related to the pseudo-second order kinetic and intraparticle diffusion were

$$\frac{t}{Q_t} = \frac{1}{kQ_e^2} + \frac{t}{Q_e} \tag{12}$$

Table 1
Physical characteristics of B, PAAm–B, Z and PAAm–Z.

	B	PAAm–B	Z	PAAm–Z
Multipoint BET surface area/$m^2\ g^{-1}$	33.4	1.65	10.4	2.75
Average pore volume/$cm^3\ g^{-1}$	0.18	0.01	0.07	0.03
Average pore diameter/nm	0.44	0.77	0.44	0.77

$$Q_t = k_i t^{1/2} \quad (13)$$

from which initial adsorption rate (Eq. (14)) and time required for adsorption of half of the concentration [26,27] (Eq. (15)) were calculated by

$$H = kQ_e^2 \quad (14)$$

$$t_{1/2} = \frac{1}{kQ_e} = \frac{Q_e}{H} \quad (15)$$

Symbols and units

$A_{i,e}$: The activity measured in initial and equilibrium solutions/cpm (counts per minute)
$C_{i,e}$: Tl concentrations at initial and equilibrium/mol L^{-1}
E: Free energy change/J mol^{-1}
F: Fractional transfer of ^{201}Tl from solution to adsorbent
H: Initial adsorption rate/mol^{-1} kg min^{-1}
k, k_i: Rate constants/mol^{-1} kg min^{-1} and mol kg^{-1} $min^{-0.5}$
K_{DR}: Constant in D–R model/mol^2 $K J^{-2}$
K_L: Langmuir adsorption equilibrium constant/L mol^{-1}
n: Freundlich constant (surface heterogeneity) related to adsorption intensity
Q: Adsorbed amounts/mol kg^{-1}
R: Ideal gas constant (8.314 J mol^{-1} K^{-1})
R_D: Dimensionless factor
T: Absolute temperature/K
$t_{1/2}$: Time required for adsorption of half of the concentration/min
V: Solution volume/L
W: Mass of adsorbent/kg
X_{DR}: DR sorption capacity/mol kg^{-1}
X_F: Freundlich constant related to adsorption capacity
X_L: Langmuir monolayer sorption capacity/mol kg^{-1}
ΔG: Change in adsorption free energy/kJ mol^{-1}
ΔH: Change in adsorption enthalpy/kJ mol^{-1}
ΔS: Change in adsorption entropy (J mol^{-1} K^{-1})
ε: Polanyi potential

3. Results and discussion

3.1. Material characterization

The minerals and composites had micro-porous structure with reference to the IUPAC classification [28] since its average pore diameters were less than <2 nm (Table 1). The encapsulation of B and Z in PAAm significantly decreased the values of BET and pore volume of these minerals, but PAAm having no porosity in its pure form attained porosity with higher pore diameters than the minerals by the inclusion of B and Z. This should be considered as an advantage in favor of the composites in view of its adsorptive features. Textural differences between PAAm and the composites were evidence for the hybrid formations of PAAm–B and PAAm–Z (Fig. 1), resembling colloidal dispersion of one solid phase (B or Z) in another (PAAm).

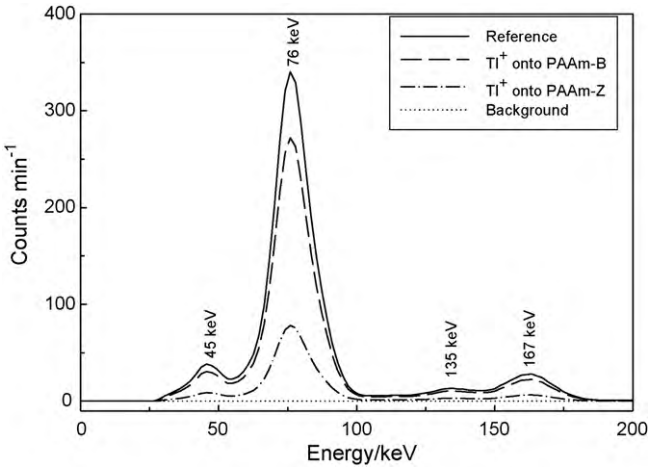

Fig. 2. Comparison of γ-spectra obtained for ^{201}Tl tagged Tl solutions before (as reference) and after adsorption of Tl onto the composites and for the background.

The γ-spectra obtained from the counts of ^{201}Tl tagged Tl^+ solutions (before and after interaction with the composites) and background were compared in Fig. 2 to visualize adsorptive features of the composites for Tl^+.

3.2. pH dependence of adsorption

The changes in adsorption of Tl as a function of the initial pH of solutions were presented in Fig. 3. The adsorbed amounts and the changes in pHs as the difference between initial and the final pH values ($\Delta pH = pH_i - pH_e$) were included in Table 2.

The amounts adsorbed onto the composites increased with increasing pH for both ions and reached a plateau around pH = 3 for Tl^+ and pH = 2 for Tl^{3+}. For both composites, the ΔpH values for Tl^+ considerably increased with increasing pH but not for Tl^{3+}.

The point of zero charge (PZC; isoelectric point) of an adsorbent is the pH of solution at which the surface of the adsorbent has zero charge. The PZC is a reference value for predication of surface charge of an adsorbent; it is positively charged at pH < PZC and negatively charged at pH > PZC. The PZC values of PAAm–B and PAAm–Z in the presence of 0.1 mol L^{-1} of KNO_3 were reported as 8.5 and 7.9 respectively [29]. In relevance to the PZC values, Xu et al. [30] assumed that the surface of aluminosilicates had amphoteric ≡SOH sites in aquatic solutions and they were either protonated to form $\equiv SOH_2^+$ or deprotonated to form $\equiv SO^-$, i.e., the $\equiv SO^-$ concentration increased with increasing pH whereas ≡SOH concentration decreased with increasing pH. This should also be the explanation of the increase observed in Tl adsorption with increasing pH;

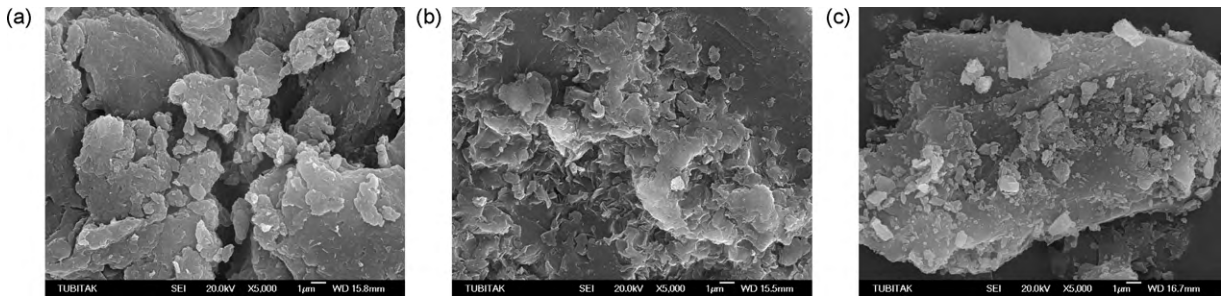

Fig. 1. SEM views of PAAm (a), PAAm–B (b) and PAAm–Z (c).

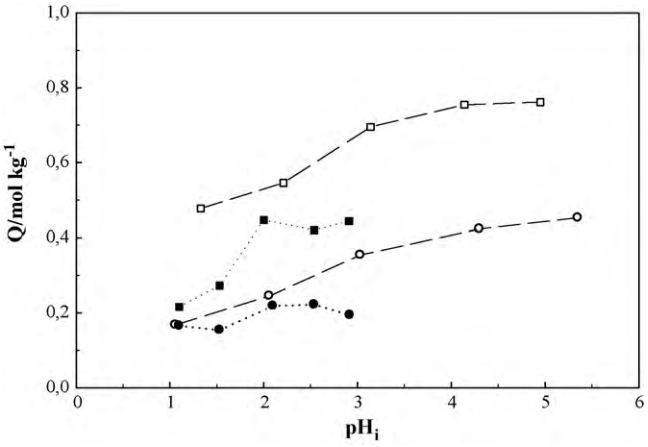

Fig. 3. Dependency of Tl^{+} and Tl^{3+} adsorption on initial pH of solutions.

the higher acidity caused the higher repulsion for the positively charged Tl ions.

By considering this and Tl^{3+} species {mononuclear $Tl(OH)^{2+}$ and $Tl(OH)_2{}^{+}$ of Tl^{3+}in acidic conditions at pH < 3 [1]}, the following adsorption mechanisms might be envisaged. The exchange (Mec. 3) should also be an explanation of the slight decrease in pH values (ΔpH < 0) for Tl^{3+} adsorption at pH = 1–2.

$$2(\equiv SO^{-}) + Tl(OH)^{2+} \rightleftarrows (\equiv SO)_2Tl(OH)_2 \quad (1)$$

$$\equiv SO^{-} + Tl(OH)_2{}^{+} \rightleftarrows \equiv SOTl(OH)_2 \quad (2)$$

$$2(\equiv SOH) + Tl(OH)^{2+} \rightleftarrows (\equiv SO)_2Tl(OH)_2 + 2H^{+} \quad (3)$$

The following exchanges could express the Tl^{+} adsorption. The mechanism 5 should be an evidence for the formations of hydroxyl bearing Tl^{+} species so that the pH of equilibrium solutions considerably increased after the adsorption.

$$\equiv SO^{-} + Tl^{+} \rightleftarrows \equiv SOTl \quad (4)$$

$$\equiv SOH^{-} + Tl(OH)_2{}^{-} \rightleftarrows \equiv SOTl + 2OH^{-} \quad (5)$$

Because of the relevance to the reusability of the adsorbents (see Section 3.6); the mechanisms (6)–(8) were additionally proposed for the recovery and reconditioning procedures.

$$\equiv SOTl + H^{+} \rightleftarrows \equiv SOH + Tl^{+} \quad (6)$$

$$\equiv SOH + H^{+} \rightleftarrows \equiv SOH_2{}^{+} \quad (7)$$

$$\equiv SOH_2{}^{+} + H_2O \rightleftarrows \equiv SOH + H_3O^{+} \quad (8)$$

3.3. Concentration dependence of adsorption

Experimentally attained adsorption isotherms and their compatibility to Langmuir, Freundlich and DR models were provided in Fig. 4. The parameters derived from the models were submitted in Table 3.

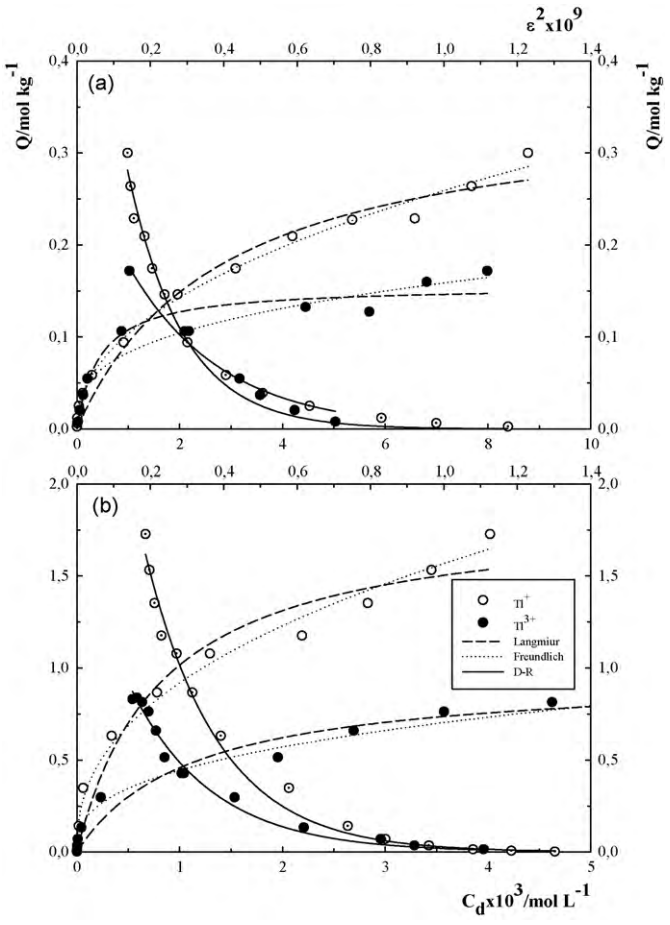

Fig. 4. Experimentally obtained Tl sorption onto PAAm–B (a) and PAAm–Z (b) and its compatibility to Langmuir and Freundlich (Q vs. Cd), and DR models (Q vs. ε^2).

The values of the adsorption capacities (X_L, X_F and X_{DR}) for Z and PAAm–Z for both ions obviously signified that the entrapping of 'Z' in PAAm remarkably improved its adsorption capacity. This should be ascribed to the fine dispersion of 'Z' particles in PAAm causing the increase in adsorptive surface and numbers of active sites available for adsorption. Although the adsorption capacity of bare 'B' was not studied due to its impractical usage in aquatic medium, the higher adsorption for PAAm–B than that for 'B' could also be envisaged. The found monolayer adsorption capacities (X_L) of PAAm–Z and PAAm–B (1.85 and 0.36 for Tl^{+} and 0.97 and 0.16 mol kg^{-1} for Tl^{3+}) were much higher than the recently reported values for Tl^{3+} onto nano-Al_2O_3 (0.03 mol kg^{-1}) and nano-TiO_2 (0.02 mol kg^{-1}) by Zhang et al. [31,32] and Tl^{+} onto sawdust treated with NaOH

Table 2
pH dependence of Tl^{+}/Tl^{3+} adsorption onto PAAm–B and PAAm–Z.

PAAm–B						PAAm–Z					
Tl^{+}			Tl^{3+}			Tl^{+}			Tl^{3+}		
pH_i	ΔpH[a]	Q[b]	pH_i	ΔpH	Q	pH_i	ΔpH	Q	pH_i	ΔpH	Q
1.0	0.0	0.18	1.1	−0.1	0.16	1.3	0.1	0.48	1.1	−0.3	0.22
2.1	0.1	0.24	1.5	−0.1	0.15	2.2	0.2	0.54	1.5	−0.2	0.27
3.0	4.2	0.36	2.1	−0.1	0.22	3.1	0.8	0.69	2.0	−0.2	0.45
4.3	4.0	0.42	2.5	0.3	0.22	4.1	1.7	0.75	2.5	0.1	0.42
5.4	3.2	0.45	2.9	0.4	0.20	4.9	1.8	0.78	2.9	0.3	0.44

[a] $pH_e - pH_i$.
[b] mol kg^{-1}.

Table 3
Langmuir, Freundlich and DR parameters for Tl^+ and Tl^{3+} adsorption onto Z, PAAm–Z and PAAm–B.

	Langmiur			Freundlich			Dubinin–Radushkevich			
	X_L [a]	K_L [b]	R^2	X_F	n	R^2	X_{DR}	K_{DR} ($\times 10^9$) [c]	E_{DR} [d]	R^2
Tl^+										
Z	0.78	1947	0.971	9.9	0.44	0.982	2.0	4.8	10.2	0.988
PAAm–Z	1.85	1220	0.972	16.7	0.42	0.992	4.1	5.0	10.0	0.990
PAAm–B	0.36	357	0.977	2.6	0.47	0.995	0.7	6.6	8.70	0.989
Tl^{3+}										
Z	0.35	131	0.896	2.1	0.42	0.937	0.6	6.3	8.90	0.946
PAAm–Z	0.97	903	0.962	5.4	0.36	0.986	1.7	4.5	10.5	0.986
PAAm–B	0.16	2258	0.945	0.8	0.33	0.947	0.3	3.9	11.3	0.978

[a] mol kg^{-1}.
[b] L mol^{-1}.
[c] mol^2 KJ^{-2}.
[d] kJ mol^{-1}.

(0.06 mol kg^{-1}) by Memon et al. [33], although the range of studied concentrations was much below than the range considered in this work.

Both composites had higher adsorption capacity for Tl^+ than that for Tl^{3+} despite the fact that Tl^{3+} shows higher tendency to form insoluble complexes than Tl^+. It gives sparingly soluble hydroxide by hydrolysis even in acidic solutions [K_{sp} of $Tl(OH)_3$ at 298 K is 6.3×10^{-46}]. Tl^{3+} has mono nuclear $Tl(OH)^{2+}$ and $Tl(OH)_2{}^+$ formations in acidic conditions at pH < 3 [1]. Beside this, Tl^+ also forms moderately soluble compounds with many anions and complex forming agents e.g. K_{sp} of TlCl at 298 K is 1.7×10^{-4}. These suggest that both ions should have affinity to the Si–O^- or Al–O^- centers on the aluminosilicate structure via complex formation or more probably ion exchange mainly Na^+/K^+. In fact, the found E_{DR} values higher than 8 kJ mol^{-1} and the mechanisms proposed (Section 3.2) indicated that the nature of adsorption was ion exchange process [34,35].

The capacity of PAAm–Z for both ions was higher than that of PAAm–B and this was obviously associated with the cation exchange capacities of the used 'Z' and 'B' (1.64 and 0.80 mol kg^{-1}). The higher tendency for adsorption of Tl^+ might be explained by the affect of ionic radii [150 pm for Tl^+ and 89 pm for Tl^{3+}, and 180 pm for $Tl(OH)^{2+}$ and 270 pm for $Tl(OH)_2{}^+$ as calculated values with reference to covalent bonding between Tl and OH with 90 nm radius] [1,36]. Contrary to expectation, the lower adsorption found for Tl^{3+} was an evidence for the formation of mono nuclear Tl^{3+} complexes at the studied pH (pH ≈ 3), the larger ions having more difficulty to pass through the holes and channels of zeolite (clinoptilolite) framework to form complexes with active sites due the to steric hindrance. Such hindrance was less possible for PAAm–B, since 'B' had a layered structure and this was intercalated with the inclusion of PAAm to 1400 pm basal spacing [20]. In fact, the studied selectivity features of the composites for both ions proved that PAAm–B had higher affinity for Tl^{3+} than Tl^+ (Section 3.7).

As 'X_L', the magnitude of a 'K_L' value (as a parameter related to spontaneity of adsorption) is also a measure of affinity of an adsorbent to an ion of interest. The sequence of found K_L values was Z > PPm-Z > PAAm–B for Tl^+ and PAAm–B > PAAm–Z > Z for Tl^{3+}, and agree with the trend seen in the values of 'n' and 'K_{DR}'. The evaluation of the values of 'X_L' together with those of 'K_L' was predicated that PAAm–Z had the higher affinity to both Tl ions than Z and PAAm–B. However, the highest value of K_L found for PAAm–B implied that the higher affinity (in terms of spontaneity) of this composite might be to Tl^{3+}, as observed in the ion selectivity study.

All values found from dimensionless analysis (R_D) of the studied initial concentrations of both ions were $0 < R_D < 1$ implying that the adsorbents were favorable for adsorption. The calculated mass of composites for 50% extraction of Tl from the hypothetical solutions containing 5×10^{-4} mol L^{-1} (100 mg L^{-1}) Tl^+ or Tl^{3+} to the solid phase by single-stage batch adsorption were 9 g L^{-1} for PAAm–B and 0.5 g L^{-1} for PAAm–Z for Tl^+, and 4 g L^{-1} for PAAm–B and 1 g L^{-1} for and PAAm–Z for Tl^{3+}. Such low amounts found especially for PAAm–Z should also be considered as an evidence for the effectiveness of this adsorbent for Tl removal.

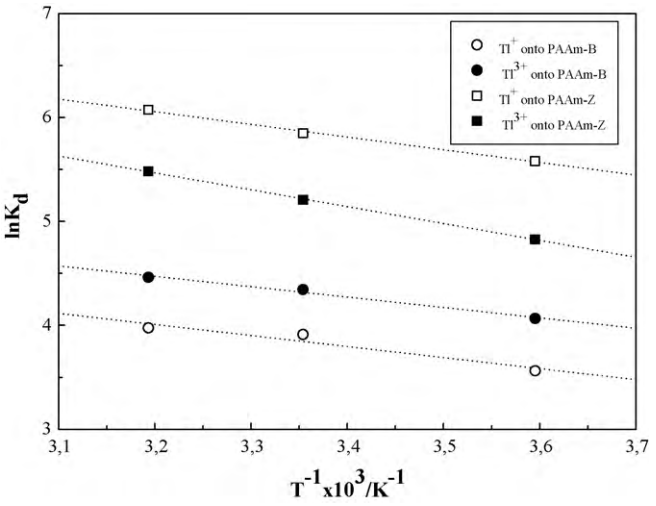

Fig. 5. Temperature dependence of Tl adsorption onto PAAm–B and PAAm–Z.

3.4. Temperature dependence of Tl adsorption

The thermodynamic parameters derived from the depictions of ln K vs. $1/T$ (Fig. 5) were introduced in Table 4.

The enthalpy and entropy changes were $\Delta H > 0$ and $\Delta S > 0$ for both ions and both composites. This indicated that the overall process was endothermic and the randomness in the solid-solution interface increased throughout the adsorption process. Gibbs free enthalpy change was $\Delta G < 0$ proving that the adsorption process was spontaneous and the spontaneity was in favor of PAAm–Z for both ions.

Table 4
Thermodynamic parameters for adsorption of Tl onto PAAm–B and PAAm–Z.

	ΔH/kJ mol^{-1}	ΔS/J mol^{-1} K^{-1}	ΔG/kJ mol^{-1}	R^2
Tl^+				
PAAm–B	8.9	62.1	−9.6	0.937
PAAm–Z	10.1	82.7	−14.5	0.996
Tl^{3+}				
PAAm–B	8.4	63.9	−10.6	0.988
PAAm–Z	13.5	88.6	−12.9	0.999

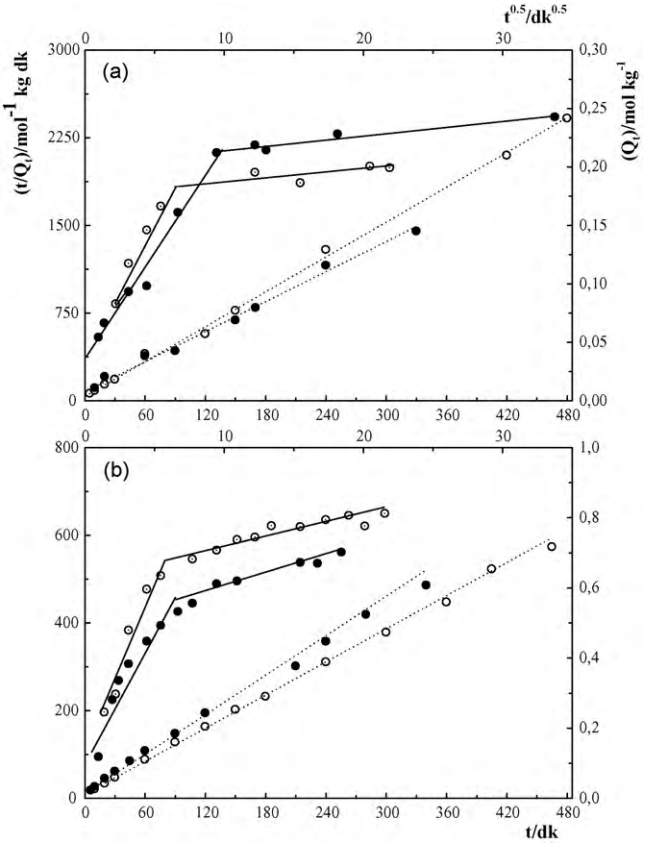

Fig. 6. Compatibility of Tl adsorption kinetics for PAAm–B (a) and PAAm–Z (b) to pseudo-second order (t/Q_t vs. t) and Weber–Morris intraparticle diffusion (Q_t vs. $t^{0.5}$) models.

3.5. Adsorption kinetics

The compatibility of experimental data to the second order kinetics and Weber–Morris intraparticle diffusion models were evaluated with reference to the statistical significance of linearity obtained from '$t-t/Q_t$' and '$t^{0.5}-Q_t$' plots (Fig. 6). The results derived from the models were provided in Table 5.

The closeness to unity of coefficients of regression attained from the second order model and identicalness of the values of adsorbed amounts at equilibrium obtained from the model (Q_e) and from the experiment (Q) eventually confirmed that the nature of adsorption was concentration dependent i.e. the rate-controlling step was chemical via ion exchange [37]. This was also consistent with the result of Weber–Morris model, '$t^{0.5}-Q_t$' plot not having intercepts at origin defining the adsorption process controlled by diffusion, but it was a curve that could be evaluated in two linear parts. While the part with a steep rise defines the initial rapid uptake by the boundary layer effects, the other resembling a plateau is associated with the intraparticle diffusion taking place after the completion of external surface coverage by the former process [38]. In fact the obtained k_i values were very low, but they implied that the contribution of diffusion process to PAAm–Z was higher than that to PAAm–B for both ions. This should also be attributable to the holed and channelled nature of zeolite unlike PAA–B with a layered structure.

The rate constants implied that the adsorption was faster in favor of PAAm–B especially for Tl^+, while the values of initial rates were higher for PAAm–Z due to its higher adsorption capacity. The values of '$t_{1/2}$' were evidence for the rapidity of the adsorption onto both composites for Tl^+ and PAAm–Z for Tl^{3+}.

3.6. Reusability

The reusability feature of PAAm–B and PAAm–Z was tested for Tl^+ for four regenerations in a total of five uses. The IR spectra obtained before and after reuses provided no evidence signifying any changes in the structures. The IR spectra taken for months with time intervals also confirmed that the storage foregoing had no effect on the structural stability.

The means and its ±SEM of the percentage adsorption and the regeneration efficiency obtained from the four following uses after the first were $28.0 \pm 0.4\%$ and $101.5 \pm 1.3\%$ for PAAm–B, and $40.1 \pm 1.8\%$ and $78.2 \pm 3.6\%$ for PAAm–Z. The mean value for PAAm–B was not significantly different from its first use (27.6%) assumed to be 100% ($p < 0.05$). The values obtained for PAAm–Z were also evidence for consistent efficiency of this material, but it was significantly different from the first (51.2%, $p > 0.05$). This was attributed to blockage of adsorptive centers or decomposition of some active sites acting as adsorbent in Z during the acidic regeneration procedure.

3.7. Tl^+/Tl^{3+} selectivity and Tl adsorption in the presence of Fe^{3+}, Pb^{2+} and Zn^{2+}

The results of ion selectivity of the adsorbents in the presence of both ions at equivalent concentrations (5×10^{-3} mol L^{-1}) indicated that PAAm–B was more selective for Tl^{3+} than PAAm–Z, but the adsorbed amounts were higher for PAAm–Z in both cases (12.7% of Tl^+ and 22.5% of Tl^{3+} for PAAm–B, and 54.4% of Tl^+ and 38.4% of Tl^{3+} for PAAm–Z).

Tl adsorption from solutions of Fe^{3+}, Pb^{2+}, Zn^{2+} at 5×10^{-3} mol L^{-1} containing Tl at equivalent, and at 5×10^{-4} and 5×10^{-5} mol L^{-1} concentrations and that from solutions

Table 5
Kinetic parameters for Tl adsorption onto PAAm–B and PAAm–Z.

	Pseudo-second order kinetic						Intrapartical diffusion	
	k[a]	Q[b]	Q_e[b]	H[c]	$t_{1/2}$[d]	R^2	k_i ($\times 10^3$)[e]	R^2
Tl^+								
PAAm–B	0.68	0.20	0.20	0.03	6.7	0.992	0.8	0.341
PAAm–Z	0.18	0.80	0.79	0.11	7.2	0.999	8.6	0.854
Tl^{3+}								
PAAm–B	0.24	0.23	0.23	0.01	23	0.978	1.3	0.942
PAAm–Z	0.21	0.68	0.67	0.09	7.4	0.992	9.8	0.972

[a] mol^{-1} kg min^{-1}.
[b] mol kg^{-1}.
[c] mol kg^{-1} min^{-1}.
[d] dk.
[e] mol kg^{-1} $min^{-0.5}$.

Table 6
Tl^+ and Tl^{3+} adsorption onto PAAm–B and PAAm–Z from Tl solutions containing Fe^{3+}, Pb^{2+} and Zn^{2+} individually and all three ions.

	Adsorption[a]/%		Adsorption[b]/%			
	5×10^{-3} mol L^{-1}		5×10^{-4} mol L^{-1}		5×10^{-5} mol L^{-1}	
	PAAm–B	PAAm–Z	PAAm–B	PAAm–Z	PAAm–B	PAAm–Z
Tl^+						
Fe^{3+}	10.3	44.5	13.4	80.4	27.2	88.7
Pb^{2+}	15.6	38.8	14.0	80.2	21.3	90.2
Zn^{2+}	17.5	49.7	20.1	93.7	42.2	97.7
M^{z+} all	7.7	43.7	16.2	80.1	13.7	87.8
Tl^{3+}						
Fe^{3+}	6.7	25.7	35.1	52.7	35.6	54.2
Pb^{2+}	21.3	20.5	42.1	67.5	45.4	62.7
Zn^{2+}	17.1	29.9	39.3	65.7	48.2	59.9
M^{z+} all	11.9	26.7	27.6	49.2	22.3	44.8

[a] From solutions M^{z+} and Tl^{z+} at equivalent concentrations.
[b] From solutions M^{z+} at 5×10^{-3} mol L^{-1} and Tl^{z+} at given concentrations.

Table 7
Tl^+ adsorption from sea water.

$[Tl^+]$/mol L^{-1}	Adsorption/%	
	PAAm–B	PAAm–Z
5×10^{-6}	7.7	13.1
5×10^{-5}	10.3	14.4
2.5×10^{-4}	14.3	23.5
5×10^{-4}	14.9	23.1

including all the competitor ions at 5×10^{-3} mol L^{-1} for each were provided in Table 6. The results showed that the presence of the foreign ions had a lowering effect on Tl adsorption for both composites, especially for Tl^+ onto PAAm–B and for Tl^{3+} on to PAAm–Z. This was attributed to the high affinity of 'B' to di- and trivalent metal ions for PAAm–B and the lowering contribution of the adsorption of competing ions for PAAm–Z. It was worth noting that Tl^+ adsorption on to PAAm–B was the lowest in the presence of Fe^{3+} and the adsorptions onto both composites were highest in the presence of Zn^{2+}. In any case, both adsorbents kept their efficacy for Tl adsorption even in the presence of all three sulfur based mineral ions. This eventually suggested that Tl could be efficiently removed from solutions/disposals of mineral processes by the use of especially PAAm–Z. This composite had 1.85 mol kg^{-1} monolayer sorption capacity for Tl^+, which was much higher than 0.84 mol kg^{-1} reported for Pb^{2+} [23].

3.8. The effect of ionic strength and Tl^+ adsorption from sea water

After adsorb ability of Tl^+ from solutions of sulfur based metal ions at various concentrations was obtained, the effect of ionic intensity was investigated for the adsorption from solutions of 10×10^{-3}–100×10^{-3} mol L^{-1} of $CaCl_2$ containing 5×10^{-3} mol L^{-1} of Tl^+. The results proved that the adsorption decreased disproportionally to the ionic intensity. The adsorption ranges were 18.0–11.4% for PAAm–B and 48.1–41.1% for PAAm–Z for which the adsorption from solutions containing Tl^+ alone were 27.6 and 51.2%. Despite the decrease, these results should still be considered as evidence for the effectiveness of the composites for Tl^+ adsorption. In fact, the results obtained from the adsorption from sea water ascertained that the composites could adsorb about 10% of Tl^+ at even 5×10^{-6} mol L^{-1} (1 mg L^{-1}) and the amounts increased to 15% for PAAm–B and 25% for PAAm–Z with increasing Tl concentrations up to 5×10^{-4} mol L^{-1} (Table 7).

4. Conclusion

In this study, adsorptive features of the PAAm–aluminosilicate composites were investigated for Tl^+ and Tl^{3+}.

Experimentally obtained isotherms were well compatible to Langmuir, Freundlich and DR models from which the derived parameters confirmed each other. The found monolayer adsorption capacities (X_L) for PAAm–Z and PAAm–B were 1.85 and 0.36 for Tl^+, and 0.97 and 0.16 mol kg^{-1} for Tl^{3+}.

The values of enthalpy and entropy changes were positive for both composites and both ions. The compatibility of adsorption kinetics to the second order and intraparticle diffusion models implied that the rate-controlling step was concentration dependent and the sorption process was ion exchange. This was also consistent with the free energy change obtained from DR model. High adsorption rates were found for both adsorbents, the time required for extracting half of Tl concentrations was 6–7 min for Tl^+.

In the presence of both ions, PAAm–B was more selective for Tl^{3+} than PAAm–Z. The reconditioning tests for both composites for Tl^+ for five uses proved that the adsorbents could be reused after complete recovery of the loaded ion. Adsorption from Tl^+ solutions containing Fe^{3+}, Pb^{2+}, Zn^{2+} confirmed that the presence of these ions had not much effect on Tl^+ extraction by especially PAAm–Z. Although Tl^+ sorption decreased with increasing ionic strength of the medium, the results obtained from the adsorption from sea water ascertained that the composites could adsorb about 10% of Tl^+ at even 5×10^{-6} mol L^{-1} (1 mg L^{-1}).

Acknowledgment

This work was supported by The Research Fund of Cumhuriyet University (CÜBAP, Project no: F-208) to which the authors are grateful.

References

[1] A.I. Busev, V.G. Tiptsova, The analytical chemistry of thallium, Russ. Chem. Rev. 29 (1960) 479–488.
[2] M. Rehkamper, S.G. Nielsen, The mass balance of dissolved thallium in the oceans, Mar. Chem. 85 (2004) 125–139.
[3] B. Venugopal, T.D. Luckey, Toxicology of non-radioactive heavy metals and their salts, in: F. Coulston, F. Korte (Eds.), Environmental Quality and Safety, Suppl. 1, Academic Pres, London, 1974, pp. 4–75.
[4] S. Galvan-Arzate, A. Santamaria, Thallium toxicity, Toxicol. Lett. 99 (1998) 1–3.
[5] A.K. Das, R. Chakraborty, M.L. Cervera, M. Guardia, Determination of thallium in biological samples, Anal. Bioanal. Chem. 385 (2006) 665–670.
[6] A.L. John Peter, T. Viraraghavan, Thallium: a review of public health and environmental concerns, Environ. Int. 31 (2005) 493–501.
[7] N.H. Chung, J. Nishimoto, O. Kato, M. Tabata, Selective extraction of thallium (III) in presence of gallium (III), indium (III), bismuth (III) and antimony (III) by salting-out of an aqueous mixture of 2-propanol, Anal Chim. Acta 477 (2003) 243–249.

[8] D.B. Nascimento, G. Schwedt, Polyethylene powder as an absorbent for preconcentration of aluminium, beryllium and thallium, Microchim. Acta 126 (1997) 159–166.
[9] M.S. Gidwani, S.K. Menon, Y.K. Agrawal, Chelating polycalixarene for the chromatographic separation Ga(III), In(III) and Tl(III), React. Funct. Polym. 53 (2002) 143–156.
[10] X. Zhang, G. Yin, Z. Hu, Extraction and separation of gallium, indium and thallium with several carboxylic acids from chloride media, Talanta 59 (2003) 905–912.
[11] N. Rajesh, M.S. Subramanian, A study of the extraction of thallium with tribenzylamine as the extractant, J. Hazard. Mater. B 135 (2006) 74–77.
[12] X. Chang, Q. Su, X. Wei, B. Wang, Synthesis and applications of poly(acrylphenylamidrazona-phenyl-hydrazide-acylphenylhydrazine) chelating fiber for preconcentration and separation of trace In(III), Zr(IV), Tl(I), V(V), Ga(III) and Ti(IV) from solution samples, Microchim. Acta 137 (2001) 209–213.
[13] A.S. Jacobson, M.B. McBride, P. Baveye, T.S. Steenhuis, Environmental factors determining the trace-level sorption of silver and thallium to soils, Sci. Total Environ. 345 (2005) 191–205.
[14] Y. Ma, W. Tong, H. Zhou, S.L. Suib, A review of zeolite-like porous materials, Micropor. Mesopor. Mater. 37 (2000) 243–252.
[15] Y.H. Wang, S.H. Lin, R.S. Juang, Removal of heavy metal ions from aqueous solutions using various low-cost adsorbents, J. Hazard. Mater. 102 (2003) 291–302.
[16] S. Babel, T.A. Kurniawan, Low-cost adsorbents for heavy metals uptake from contaminated water, J. Hazard. Mater. 97 (2003) 219–243.
[17] P.F. Luckham, S. Rossi, The colloidal and rheological properties of bentonite suspensions, Adv. Colloid Interface Sci. 82 (1999) 43–92.
[18] A. Godelitsas, T. Armbruster, HEU-type zeolites modified by transition elements and lead, Micropor. Mesopor. Mater. 61 (2003) 3–24.
[19] S.G. Stradoubtsev, A.A. Ryabova, A.R. Khokhlov, Composite gels of poly(acrylamide) with incorporated bentonite. Interaction with cationic surfactants, ESR and SAXS study, Macromolecules 35 (2002) 6362–6369.
[20] U. Ulusoy, S. Şimşek, Ö. Ceyhan, Investigations for modification of polyacrylamide-bentonite by phytic acid and its usability in Fe^{3+}, Zn^{2+} and $UO_2{}^{2+}$ adsorption, Adsorption 9 (2003) 165–175.
[21] U. Ulusoy, S. Şimşek, Ö. Ceyhan, Adsorption of $UO_2{}^{2+}$, Tl^{+}, Pb^{2+}, Ra^{2+} and Ac^{3+} onto polyacrylamide–bentonite composite, J. Radioanal. Nucl. Chem. 256 (2003) 315–321.
[22] S. Şimşek, U. Ulusoy, $UO_2{}^{2+}$, Tl^{+}, Pb^{2+}, Ra^{2+}, Bi^{3+} and Ac^{3+} adsorption onto polyacrylamide-zeolite composite and its modified composition by phytic acid, J. Radioanal. Nucl. Chem. 261 (2004) 79–86.
[23] U. Ulusoy, S. Şimşek, Lead removal by polyacrylamide–bentonite and zeolite composites: effect of phytic acid immobilization, J. Hazard. Mater. B 127 (2005) 163–171.
[24] U. Karlsson, A. Düker, S. Karlsson, Separation and quantification of Tl(I) and Tl(III) in fresh water samples, J. Environ. Sci. Heal. A 41 (2006) 1155–1167.
[25] M. Doğan, M. Alkan, Removal of methyl violet from aqueous solution by perlite, J. Colloid Interface Sci. 267 (2003) 32–41.
[26] Y.S. Ho, G. Mckay, Pseudo-second order model for sorption processes, Process Biochem. 34 (1999) 451–461.
[27] S. Basha, Z.V.P. Murthy, Kinetic and equilibrium models for biosorption of Cr(VI) on chemically modified seaweed, *Cystoseira indica*, Process Biochem. 42 (2007) 1521–1529.
[28] K.S.W. Sing, D.H. Everett, R.A.W. Haul, L. Moscou, R.A. Pierotti, J. Rouquerol, T. Siemieniewska, Reporting physisorption data for gas/solid systems with special reference to the determination of surface area and porosity, Pure Appl. Chem. 57 (1985) 603–619.
[29] D. Baybaş, The characterization of polyacrylamide-aluminosilicate composites and the investigation for their adsorptive features for thorium, Ph.D. Thesis, Cumhuriyet University, Sivas, Turkey, 2009.
[30] D. Xu, C. Chen, X. Tan, J. Hu, X. Wang, Sorption of Th(IV) on Na-rectorite: effect of HA, ionic strength, foreign ions and temperature, Appl. Geochem. 22 (2007) 2892–2906.
[31] L. Zhang, T. Huang, M. Zhang, X. Guo, Z. Yuan, Studies on the capability and behavior of adsorption of thallium on nano-Al_2O_3, J. Hazard. Mater. 157 (2008) 352–357.
[32] L. Zhang, T. Huang, N. Liu, X. Liu, Sorption of thallium(III) ions from solutions using titanium dioxide nanoparticles, Microchim. Acta 165 (2009) 73–78.
[33] S.Q. Memon, N. Memon, A.R. Solangi, J.R. Memon, Sawdust:, A green and economical sorbent for thallium removal, Chem. Eng. J. 140 (2008) 235–240.
[34] B.S. Krishna, B.S. Murty, J. Prakash, Thermodynamics of chromium(VI) anionic species sorption onto surfactant-modified montmorillonite clay, J. Colloid Interface Sci. 229 (2000) 230–236.
[35] A.R. Cestari, E.F.S. Vieira, C.R.S. Mottos, Thermodynamics of Cu(II) adsorption thin vanilin-modified chitosan membranes, J. Chem. Thermodyn. 38 (2006) 1092–1099.
[36] N.N. Greenwood, A. Earnshaw, Chemistry of the Elements, Butterworth-Heinemann Ltd., Cambridge, 1995.
[37] U. Ulusoy, R. Akkaya, Adsorptive features of polyacrylamide–apatite composite for Pb^{2+}, $UO_2{}^{2+}$ and Th^{4+}, J. Hazard. Mater. 163 (2009) 98–108.
[38] Y. Khambhaty, K. Mody, S. Basha, B. Jha, Kinetics, equilibrium and thermodynamic studies on biosorption of hexavalent chromium by dead fungal biomass of marine *Aspergillus niger*, Chem. Eng. J. 145 (2009) 489–495.